RSC Advances

This is an *Accepted Manuscript*, which has been through the Royal Society of Chemistry peer review process and has been accepted for publication.

Accepted Manuscripts are published online shortly after acceptance, before technical editing, formatting and proof reading. Using this free service, authors can make their results available to the community, in citable form, before we publish the edited article. This *Accepted Manuscript* will be replaced by the edited, formatted and paginated article as soon as this is available.

You can find more information about *Accepted Manuscripts* in the **Information for Authors**.

ROYAL SOCIETY OF CHEMISTRY

www.rsc.org/advances

Simple and efficient protocol for synthesis of pyrido [1, 2-*a*] pyrimidin-4-one derivatives over solid heteropolyacid catalysts

Sulaiman N. Basahel[1,2], Nesreen S. Ahmed[1,3*], Katabathini Narasimharao[1,2*], Mohamed Mokhtar[1,2]

1.Chemistry Department, Faculty of Science, King Abdulaziz University, Jeddah 21589, P.O. Box 80203, Saudi Arabia
2. Surface Chemistry and Catalytic Studies Group, King Abdulaziz University, Jeddah, Saudi Arabia
3. Medicinal Chemistry Department, National Research Centre, El Buhouth St. Dokki, Cairo, Egypt

Abstract

Aluminium exchanged tungstophosphoric acid salts with Keggin structure ($Al_xH_{3-x}PW_{12}O_{40}$) were prepared by simple ion exchange method. The prepared heteropolyacid salts were characterized by various techniques such as elemental analysis, XRD, FTIR, UV-*vis*, N_2-physisorption, NH_3-TPD and FTIR-pyridine adsorption. All the prepared catalysts possess both Brönsted and Lewis acid sites, however increase of surface area and Lewis acid sites was observed with increase of Al content. The catalysts have been applied as heterogeneous catalysts to synthesize pyrido [1,2-*a*] pyrimidines under mild reaction conditions. A variety of biologically active pyrido[1,2-*a*] pyrimidines were obtained in best yields ever (above 90%) by using a simple, eco-friendly and efficient protocol catalyzed by $Al_xH_{3-x}PW_{12}O_{40}$ catalysts. $Al_3PW_{12}O_{40}$ catalyst showed highest activity due to introduction of more number of Lewis acid sites to parent $H_3PW_{12}O_{40}$ by complete exchange of H^+ ions by Al^{3+} ions.

Keywords: Pyrido [1, 2-*a*] pyrimidin-4-one; Solid heteropolyacid; $Al_xH_{3-x}PW_{12}O_{40}$; Efficient protocol

*Corresponding Authors, Fax: +966-26952292; Tel: +966-538638994;
E-mail: nkatabathini@kau.edu.sa (Narasimharao); nesreen69eg@yahoo.com (Nesreen)

1

1. Introduction

The pyrimidine core has always attracted much attention as compounds containing this structural motif are known to exhibit diverse pharmaceutical potency. The purine bases of DNA and RNA as well as the building blocks of numerous natural products known to have the pyrimidine unit [1]. It was reported that pyrido [1,2-*a*] pyrimidine derivatives are useful building blocks for the synthesis of well-known drugs [Fig. 1] such as antipsychotic agents [2] antiasthmatic agent [3], tranquilizer [4], anti-allergic and antiulcerative agents [5].
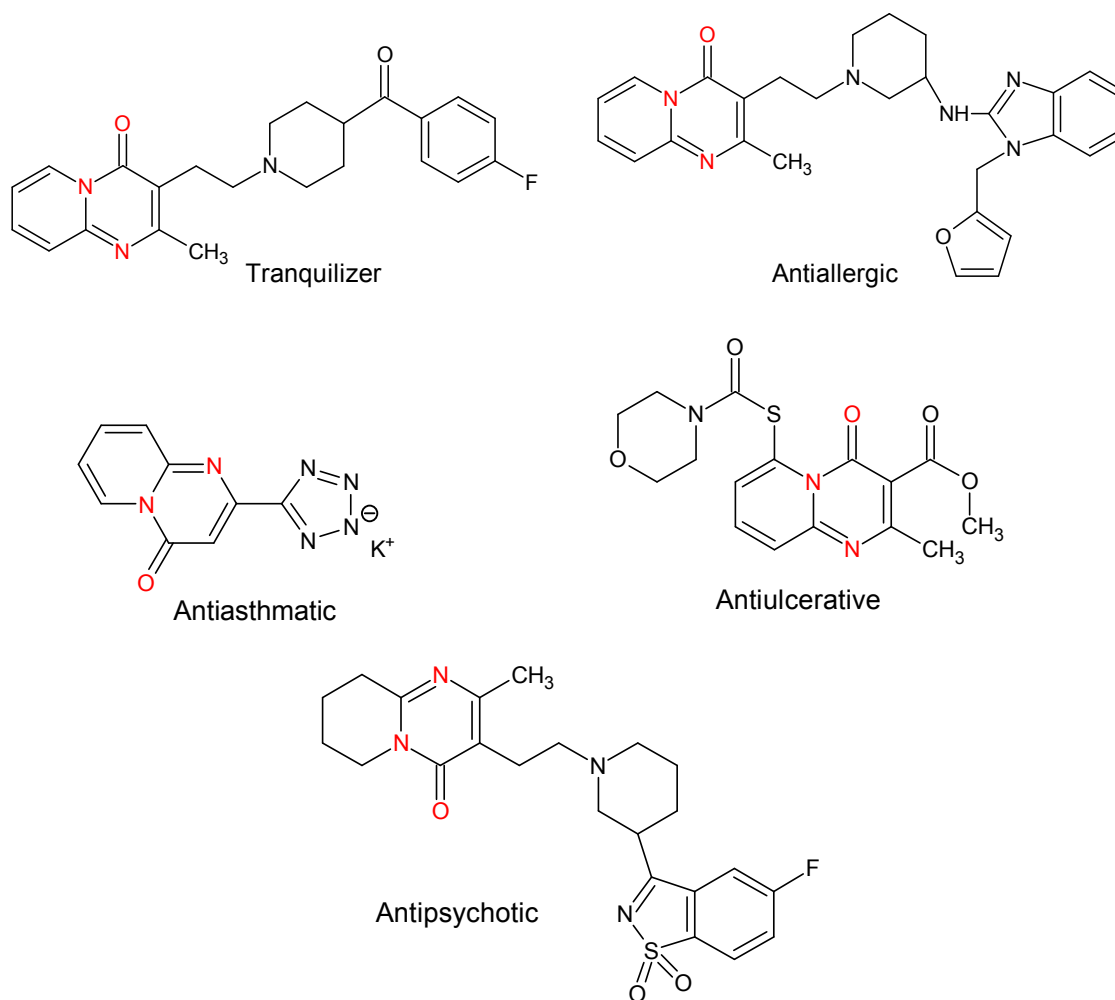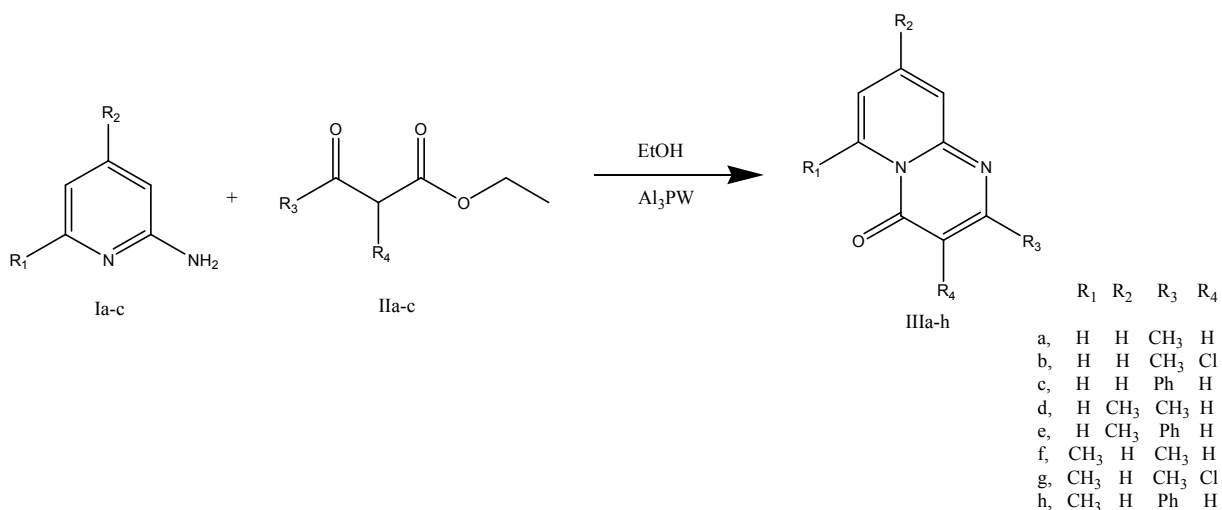

Fig. 1: Few examples of biologically active agents consisted of pyrido [1,2-*a*] pyrimidine derivatives

A vast number of methods have been developed for the synthesis of pyridopyrimidine derivatives [6]. The pyrido[1,2-*a*]pyrimidin-4-ones (Scheme 1) forms the best-known class of pyrido[1,2-*a*]pyrimidines, to which numerous synthetic routes are available [7], however, the reported methods usually requires longer reaction time, complex synthetic methodologies, expensive homogeneous catalyst and often used harmful organic solvents.

	R_1	R_2	R_3	R_4
a,	H	H	CH_3	H
b,	H	H	CH_3	Cl
c,	H	H	Ph	H
d,	H	CH_3	CH_3	H
e,	H	CH_3	Ph	H
f,	CH_3	H	CH_3	H
g,	CH_3	H	CH_3	Cl
h,	CH_3	H	Ph	H

Scheme 1: Synthesis of pyrido[1,2-*a*]pyrimidin-4-one derivatives **III**_**a-h**

Reported literature methods to synthesize pyrido [1,2-*a*] pyrimidin-2-ones involved different methodologies. Roma et al. [8] obtained a mixture of pyrido [1,2-*a*] pyrimidin-2-ones and pyrido [1,2-*a*] pyrimidin-4-ones by performing the cyclization of 2-aminopyridine with the Vilsmeier-Haack reagent which prepared in situ from *N*-alkyl-*N*-arylethoxycarbonylacetamide and phosphorus oxychloride was used as catalyst. Doad et al. synthesized of derivatives of pyrido [1, 2-*a*] pyrimidin-2-ones by the reaction of 2-aminopyridines with allene-1,3- dicarboxylic esters [9]. Dotokhov et al. [10] reported the cyclization of 2-aminopyridine with ethyl cyanoacetate at 80-100 °C under 14 kbar pressure. Suri et al. [11] used acid catalyzed cyclization of *N*-acetoacetylated 2-amino

3

pyridines/picolines/quinolines under microwave irradiation. Formation of significant amount of undesired products was observed when the reaction was carried out between 2-aminopyridine and phenylpropiolic ester [12]. Thus exploration of more simple and convenient synthetic method for the synthesis of pyrido [1, 2-*a*] pyrimidin-2-ones still remains an active research area.

Keggin structured heteropoly compounds are known to possess high acidity and oxidizing properties. These materials can be used to replace classical mineral acids with some advantages, such as a lower corrosion and a lower production of wastes, thus leading to eco-efficient processes [13]. The bulk heteropolyacids, such as tungstophosphoric and tungstosilicic acids, lead to low catalytic yield in some acid reactions, mainly due to their low specific surface area. This disadvantage can be overcome by using their salts with different cations or supporting the heteropolyacid on adequate porous supports [14]. The acidic properties of the salts of the heteropolyacids depend on the cation type, the constituent elements of the polyanion and their tertiary structure [15]. The partial hydrolysis and the presence of in homogeneities resulting from the synthesis also exert a marked influence. The salts of the Keggin heteropolyacids can be classified into two groups [16]. The salts of small cations (classified as type A) are very soluble in water or organic solvents, possess a low specific surface area, and in general behave in many respects in a similar way to the parent acid. The salts of large cations (classified as type B) are insoluble in water, have high specific surface area and relatively high thermal stability. The salts of large cations gave excellent catalytic activity in diverse acid reactions [17]. However, the salts of the A type have been less utilized. The salts of the Al^{3+} cation of the tungstophosphoric acid (AlPW) have interesting

characteristics for their use as catalysts because they can present Lewis and/or Brönsted acid sites. Baba et al. [18] studied the generation of acidic sites in the Al^{3+} and Cu^{2+} neutral salts of tungstophosphoric acid. Firouzabadi et al. [19] have studied the effect of the non-hygroscopic $AlPW_{12}O_{40}$ salt in the acylation of aromatic compounds.

Previous reports have also suggested that synthesis of pyrido [1, 2-*a*] pyrimidines process can be successfully carried out by various Lewis acidic catalysts. In view of these considerations, it is interesting to study the exchange of Al with HPW as it generates the Lewis acidic sites over the catalyst surface, whereby the rate of the reaction would be increased significantly as compared to that of parent H_3PW catalyst. Therefore, it is our aim to test the scope for synthesis of pyrido [1, 2-*a*] pyrimidine derivatives using AlPW catalyst (Scheme 1). In our continued interest in the development of highly expedient methods for the synthesis of important organic derivatives [20] we report in this paper a simple and convenient synthesis protocol for synthesis of pyrido [1,2-*a*] pyrimidine derivatives catalyzed by solid Keggin structured AlPW catalysts. The objective of this work is to prepare and characterize the AlPW salts and apply them as catalysts to obtain pyrido [1, 2-*a*] pyrimidine derivatives in higher yields and correlate the characteristic properties of AlPW catalysts with their catalytic activity.

2. Experimental

2.1 Preparation of Al salts of tungstophosphoric acid

First, tungstophosphoric acid (H_3PW) was dried at 100 ^{o}C to remove the physically adsorbed water before use. $Al_xH_{3-x}PW_{12}O_{40}$ samples (x = 1, 2 and 3) were prepared by dropwise addition of predetermined amounts of a 0.02 mol dm^{-3} aluminum

nitrate aqueous-ethanol (50:50 volume ratio) solution to a 0.08 mol dm^{-3} ethanol solution

of tungstophosphoric acid at room temperature. The obtained white precipitate was left to

dry overnight at room temperature in a vacuum oven to remove the ethanol and water.

Fine white powders were obtained by oven-drying the materials in air at 100 $^{\circ}$C. No

further pretreatments were applied to the materials, which were stored in air before

analysis and reaction testing. Catalysts are abbreviated with reference to their Al content

(e.g., $Al_2 = Al_2HPW_{12}O_{40}$). The extent of proton exchange by Al and final composition of

the salts were determined by elemental analysis (Table 1).

2.2 Characterization of catalysts

X-ray powder diffraction (XRD) studies were performed for all of the prepared

solid samples using a Bruker diffractometer (Bruker D8 advance target). The patterns

were run with copper Kα and a monochromator (λ= 1.5405 Å) at 40 kV and 40 mA. The

crystallite size of the MgSil phase was calculated using Scherrer's equation:

$$D = B\lambda/ \beta_{1/2} \cos \theta \qquad (1)$$

where D is the average crystallite size of the phase under investigation, B is the Scherer

constant (0.89), 'λ' is wavelength of the X-ray beam used (1.54056 Å), '$\beta_{1/2}$' is the full

width at half maximum (FWHM) of the diffraction peak and 'θ' is the diffraction angle.

The identification of different crystalline phases in the samples was performed by

comparing the data with the Joint Committee for Powder Diffraction Standards (JCPDS)

files.

FTIR spectra of catalysts obtained at room temperature using Perkin-Elmer

Spectrum 100 FTIR spectrometer. Then, the samples were subjected to pyridine

adsorption analysis. The analysis was carried out over a catalyst coated on a silicone disk

which was treated under vacuum for 5 h. Later, the samples were treated with pyridine vapor and finally heated at 100 ^{o}C under vacuum for 30 min. The amount of Brönsted and Lewis acid sites was calculated *via* integration of the area of the absorption bands showing the maximum values of intensity at 1446 cm^{-1} and 1536 cm^{-1}, respectively. Integrated absorbance of each band was obtained using the appropriate software by applying the corresponding extinction coefficient and normalized by the weight of the samples.

DR UV-*vis* absorption spectra of the samples were collected using a Thermo-Scientific evolution spectrophotometer equipped with an integrating sphere in the wavelength range 200-800 nm to measure the reflectance spectra of each sample. A small amount (10 mg) of the sample in powder form was dispersed and pressed firmly between two microscope glass plates to create a thin absorbing film.

The textural properties of the synthesized samples were determined from nitrogen adsorption/desorption isotherm measurements at -196 ^{o}C using a model NOVA 3200e automated gas sorption system (Quantachrome, USA). Prior to measurement, each sample was degassed for 6 h at 150 ^{o}C. The specific surface area, S_{BET}, was calculated by applying the Brunauer-Emmett-Teller (BET) equation. The average pore radius was estimated from the relation $2V_p/S_{BET}$, where V_p is the total pore volume (at $P/P^0 = 0.975$). Pore size distribution over the mesopore range was generated by the Barrett-Joyner-Halenda (BJH) analysis of the desorption branches, and the values for the average pore size in radius were calculated.

The acidity of the samples were further characterized by temperature programmed desorption (TPD) using 99.9% NH_3/He. TPDs were performed in a Quantachrome

CHEMBET 3000 apparatus coupled to a thermal conductivity detector. Sample (0.1 g) was pretreated under the flow of helium gas [25 ml min^{-1}, 99.99%] at 200 °C for 1 hour. Sample was then cooled to 30 °C and saturated the sample with of NH_3 (50 ml min^{-1}) for 1 hour. The loosely bound NH_3 to the sample surface was removed by flowing helium gas (50 ml min^{-1}) for 1 hour. The NH_3-TPD patterns were recorded by increasing the temperature of the sample at 10 °C min^{-1} up to 800 °C.

2.3 Typical procedure for the synthesis of pyrido[1,2-*a*]pyrimidin-4-ones

Solid catalyst (0.1 g), was added to a mixture of 2-amino-6-methylpyridine **I** (1.08g, 10 mmol) and 1, 3 diketone derivatives **II$_{a-c}$** (10 mmol) in absolute ethanol (10 ml), and then the reaction was started at refluxing temperature. The progress of the reaction was monitored by TLC. Upon completion of the reaction, the mixture was filtered on hot to extract the solid catalyst. Dissolution of the products in hot alcohol after evaporating the volatile materials by vacuum, compounds **III$_{a-h}$** were re-crystallized. The used catalyst was collected by washing with hot ethyl alcohol.

2.4 Analyses of the reaction products

All melting points were measured on a Gallenkamp melting point apparatus and are uncorrected. The infrared spectra were recorded for the compounds in Perkin Elmer SP 100 infrared spectrophotometer. The ^1H NMR and ^{13}C NMR spectra were recorded on a Bruker WM-600 and WM 350 MHz spectrometer, receptively using TMS (0.00 ppm). The signal of the deuterated solvents was used as internal standard. Chemical shifts (δ) are given in ppm relative to the signal for TMS as a standard, and coupling constant in Hz. Mass spectra were recorded on a Shimadzu GCMS-QP 1000 EX mass spectrometer at 70 eV. Elemental analyses (C, H, N and S) were carried out at the Microanalytical

Center of Cairo University, Giza, Egypt, the results were found to be in good agreement (±0.3%) with the calculated values.

2-Methyl-4H-pyrido [1, 2-a] pyrimidin-4-one

(III$_a$)Yellow crystals from ethanol and n-hexane (3:1), m.p. 120-122°C [Ref. [21] m.p. 118-119°C], FTIR v_{max}/cm^{-1}: 1668 (C=O); ^{1}HNMR (CDCl$_3$): δ 2.42 (s, 3H, 2-CH$_3$), 6.30 (s, 1H, H-3), 7.07 (t, 1H, J = 9, H-8,), 7.54 (d, 1H, J = 13.2, H-9), 7.68 (t, 1H, J =7.2, H-7),9.00 (d, J=10.8, H-6). ^{13}C NMR (CDCl$_3$): δ 24.7, 103.4, 115.0, 125.8, 127.3, 136.2, 150.7, 157.9, 165.3; MS (m/z): 160(M$^+$).

3-Chloro-2-methyl-4H-pyrido [1, 2-a] pyrimidin-4-one

(III$_b$)Yellow crystals from ethanol, m.p. 187-189°C [Ref. [22] m.p. 186-187°C], FTIR v_{max}/cm^{-1}: 1705 (C=O); ^{1}HNMR (CDCl$_3$): δ 2.61 (s, 3H, 2-CH$_3$),7.15 (t, 1H, J = 8.4, H-8,), 7.59 (d, 1H, J = 13.2, H-9), 7.71 (t, 1H, J =7.2, H-7), 9.00 (d, J=10.2, H-6). ^{13}C NMR (CDCl$_3$): δ 23.3, 111.7, 115.9, 125.9, 127.5, 135.9, 148.1, 154.4, 161.7; MS (m/z): 194.5(M$^+$), 196.5 (M$^+$+2).

2-Phenyl-4H-pyrido [1, 2-a] pyrimidin-4-one

(III$_c$)Yellow powder from ehanol, m.p. 146-148°C [Ref. [21] m.p. 144-145°C], FTIR v_{max}/cm^{-1}: 1683(C=O); ^{1}HNMR (CDCl$_3$): δ 6.89 (s, 1H, H-3), 7.11 (t, 1H, J = 7.2, H-8,), 7.72 (d, 1H, J = 11.4, H-9), 7.74 (t, 1H, J =7.2, H-7),9.05 (d, 1H, J=10.8, H-6), 7.47,8.07 (2m, 5H, Ph-H) . ^{13}C NMR (CDCl$_3$): δ 100.1, 115.3, 126.7, 127.3, 127.5, 128.9, 130.7, 136.3, 137.2, 151.0, 158.6, 162.0; MS (m/z): 225(M$^+$).

2, 8-Dimethyl-4H-pyrido [1, 2-a] pyrimidin-4-one

(III$_d$)Yellow crystals from pet-ether 60-80°, m.p. 129-131°C [Ref. [23] m.p. 130-132°C], FTIR v_{max}/cm^{-1}: 1667 (C=O); ^{1}HNMR (CDCl$_3$): δ 1.92,2.42 (2s, 6H, 2-CH$_3$), 6.24 (s,

1H, H-3), 6.93 (d, 1H, J = 11.4, H-7,), 7.39 (s, 1H, H-9), 8.89 (d, 1H, J =11.4, H-6). [13]C

NMR (CDCl$_3$): δ 21.5, 24.5, 102.4, 117.9, 123.7, 126.6, 148.8, 150.6, 157.8, 165.2; MS

(*m/z*): 162(M$^+$).

8-Methyl-2-phenyl-4H-pyrido [1, 2-a] pyrimidin-4-one

(**III$_e$**) Beige crystals from carbon chloroform, m.p. 139-141°C [Ref. [23] m.p. 138-

139°C], FTIR v_{max}/cm^{-1}: 1694 (C=O); ^{1}HNMR (CDCl$_3$): δ 2.49 (s, 3H, CH$_3$), 6.59 (s,

1H, H-3), 7.15 (d, 1H, J = 12, H-7,), 7.24 (s, 1H, H-9), 8.54 (d, 1H, J =12, H-6), 7.46,7.65

(2m , 5H, Ph-H). ^{13}C NMR (CDCl$_3$): δ 109.6, 118.0, 120.6, 126.6, 129.5, 131.1, 134.0,

136.1, 150.1, 150.3, 163.1, 178.9; MS (*m/z*): 239(M$^+$)

2, 6-dimethyl-4H-pyrido [1, 2-a] pyrimidin-4-one

(**III$_f$**)Yellow crystals, m.p. 85-87°C [Ref. [24] m.p. 85∘C], FTIR v_{max}/cm^{-1}: 1662 (C=O);

^{1}HNMR (CDCl$_3$): δ 2.36 (s, 3H, 2-CH$_3$), 3.04 (s, 3H, 6-CH$_3$), 6.16 (s, 1H, H-3), 6.62 (d,

1H, J = 6.6, H-7), 7.33 (d, 1H, J = 9, H-9), 7.41 (dd, 1H, J=6.6 ,9 , H-8). ^{13}C NMR

(CDCl$_3$): δ 24.0, 24.9, 105.8, 188.1, 124.9, 135.4, 144.1, 153.4, 162.2, 163.5; MS (*m/z*):

174(M$^+$).

3-chloro-2, 6-dimethyl-4H-pyrido [1, 2-a] pyrimidin-4-one

(**III$_g$**) Pale brown crystals, m.p. 196-197°C [Ref. [25] m.p. 195-196°C], FTIR v_{max}/cm^{-1}:

1712 (C=O); ^{1}HNMR (CDCl$_3$): δ 2.56 (s, 3H, 2-CH$_3$), 3.10 (s, 3H, 6-CH$_3$), 6.71 (d, 1H, J

= 7.2, H-7), 7.38 (d, 1H, J = 9 , H-9), 7.44 (d, 1H, J =7.2, 9, H-8). ^{13}C NMR (EtOD): δ

19.8, 24.9, 110.0, 117.4, 121.0, 135.5, 151.3, 153.0, 164.2, 180.1; MS (*m/z*): 208(M$^+$),

210(M$^+$+2).

6-methyl-2-phenyl-4H-pyrido [1, 2-a] pyrimidin-4-one

(**III$_h$**) light yellow crystals, m.p. 143-145°C [Ref. [26] m.p. 142-145$^°$C], FTIR v_{max}/cm^{-1}:

1667 (C=O); ^{1}HNMR (CDCl$_3$): δ 3.10 (s, 3H, 6-CH$_3$), 6.65 (d, 1H, J = 6.6 H-7), 6.74 (s,

1H, C$_3$-H),7.43 (d, 1H, J = 8.4, H-9), 7.49 (m,5H,Ph-H), 8.07(dd, 1H, J$_{7,8}$ =6.6,8.4, H-8).

^{13}C NMR (CDCl$_3$): δ 24.8, 109.8, 118.1, 120.8, 126.8, 129.7, 131.3, 134.2, 136.3, 150.3,

150.5, 163.3, 179.2; MS (*m/z*): 236(M$^+$).

3. Results and discussion

3.1 Elemental analysis

The bulk and surface composition of the parent H$_3$PW and AlPW samples were

performed by elemental and XPS analysis respectively. Good agreement between

nominal and observed bulk Al content was observed for all the samples (Table 1). The

results show that the surface composition varies with increasing bulk Al content from 3.9

to 12.5 wt%. The almost linear increase in surface Al and concomitant decrease in

surface W confirms the incorporation of Al into the H$_3$PW clusters rather than simple

encapsulation of H$_3$PW particles with Al over layer. The surface Al content is slightly

lower than the bulk, suggesting that the surface is Al-depleted. The bulk and theoretical

values are in excellent agreement; however, there is a significant deviation between the

surface and bulk Al/W ratios at low Al content. This kind of deviation was previously

observed by other authors and consistent with the reports for the metal (M) salts of

H$_3$PW. The observed deviation was accounted for by structural models proposed for

intermediate M$_x$H$_{3-x}$PW$_{12}$O$_{40}$ compositions, in which M$_3$PW$_{12}$O$_{40}$ core particles

purportedly are coated with a surface layer of H$_3$PW$_{12}$O$_{40}$ clusters [27]

Table 1: Elemental composition and crystallite size of catalysts

Catalyst	Crystallite size (nm)	Bulk elemental composition (wt%)[a]		Surface elemental composition (wt%)[b]	
		Al	W	Al	W
H₃PW	80	-	77	-	76
AlH₂PW	64	3.9	75.4	1.1	71
Al₂HPW	30	8.4	69	6.8	67.9
Al₃PW	40	12.5	66	11.9	64.8

[a] AAS analysis by dissolving the salts in standard NaOH solution
[b] XPS analysis

3.2 X-ray diffraction

X-ray powder diffraction is commonly used to study the structure of heteropoly compounds. The powder XRD patterns of all the samples are shown in Fig. 2. Pure H₃PW sample exhibits all of the reflections corresponding to a cubic *Pn3m* crystalline structure [28]. After initial ion-exchange to form $AlH_2PW_{12}O_{40}$, a new set of peaks evolved; the diffraction peaks corresponding to the free acid disappeared as the Al content increased to 2 and 3. The shift in H₃PW peaks toward higher angles in the AlPW samples is consistent with the body-centered cubic (bcc) structure of $Al_3PW_{12}O_{40}$ salts reported in the literature [29] and the observed XRD results indicate the presence of a unique crystalline $Al_3PW_{12}O_{40}$ phase in all AlPW samples. From X-ray peak broadening, it is possible to calculate the average particle size of the phases using Scherrer's equation. The crystallite size (*D* in diameter) of the AlPW samples, summarized in Table 1, was calculated from this equation (1). Analysis of the line widths of the XRD peaks of the Al_xPW salts (*x* = 0-3) show that the size of the primary crystallites decrease from 80 to 30 nm as Al loading increases to Al₂, and particle size increases to 40 nm for the Al₃ sample, indicating the formation of aggregates of the Al₃PW core at high Al loading.
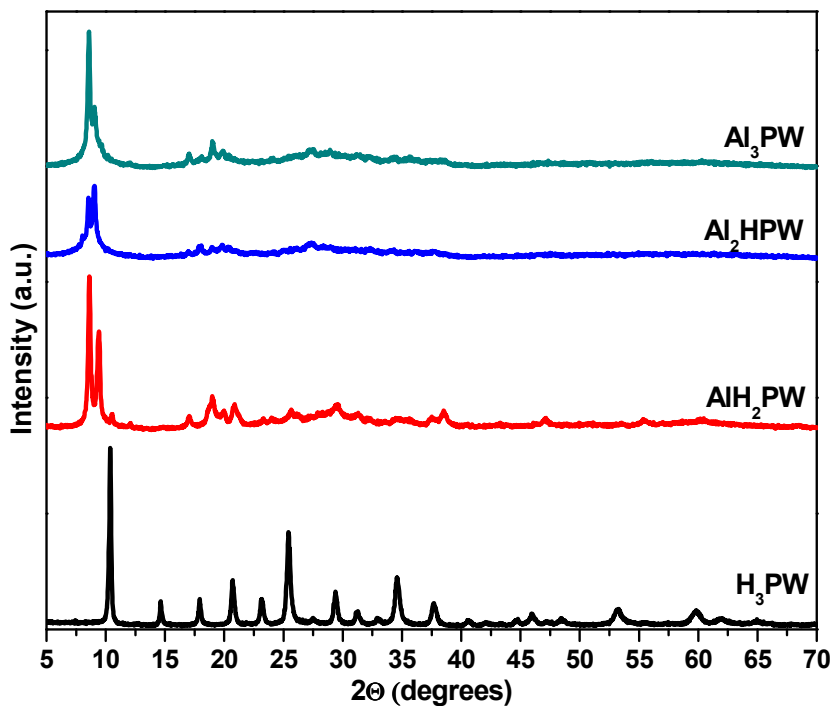
Fig 2: XRD patterns of all the samples

3.3 FTIR spectroscopy

FTIR spectra have proved to be a powerful technique to study the changes in the primary, secondary and tertiary structures of the heteropoly compounds. The FTIR spectrum of H_3PW sample showed bands at 1080, 981, 886, 791, 593, and 525 cm^{-1}, which corresponds to the $P-O_a$, $W=O_d$, $W-O_b-W$, $W-O_c-W$ stretching vibrations, and to O_a-P-O_a deformation, respectively and they are in accordance with those reported in the literature for the H_3PW [30]. The subscripts correspond to oxygen atoms binding W and P (a), or bridging different WO_6 octahedra that share corners (b) or edges (c), and terminal oxygen atoms and (d) bonded to only one W atom; similar FTIR spectra were found for all the AlPW samples (Fig.3).

13
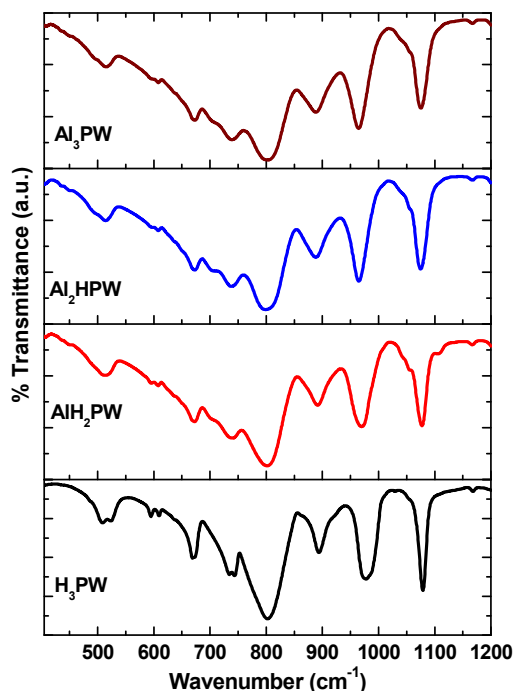
Fig. 3: FTIR spectra of all the samples

It can observed that the band assigned to the $W=O_d$ stretching for AlPW samples is broadened as a result of the interaction between the $[PW_{12}O_{40}]^{3-}$ anion and Al^{3+} cations. However, transformation of the Keggin species; $[PW_{12}O_{40}]^{3-}$ into the lacunary Keggin phase; $[PW_{11}O_{39}]^{7-}$ during the preparation was not detected for all the AlPW salts. These results indicating that the primary Keggin structure of all the prepared samples still remained intact after the partial or full substitution of Al ions, even though XRD patterns of the AlPW samples showed some differences.

3.4 Diffuse reflectance UV-*vis* spectroscopy

Fig. 4 shows the diffuse reflectance UV-*vis* spectra for all the samples. Two main absorptions are present in the spectrum of parent H_3PW sample; the first is centered at 260 nm. In the diffuse reflectance spectra of pure heteropoly acids the main absorption band in the UV-*vis* range is due to the ligand-metal charge transfer (LMCT): $O_2 \rightarrow W^{6+}$. This type of transition usually observed between 200 and 400 nm [31], thus the transition

at 260 nm could be attributed to the oxygen-tungsten charge-transfer absorption band for Keggin anions. Another LMCT broad band centered at 360 nm was observed for the H_3PW sample. For the AlPW samples, these bands are clearly shifted to lower wavelengths and the bands were observed at 230 and 310 nm, respectively.
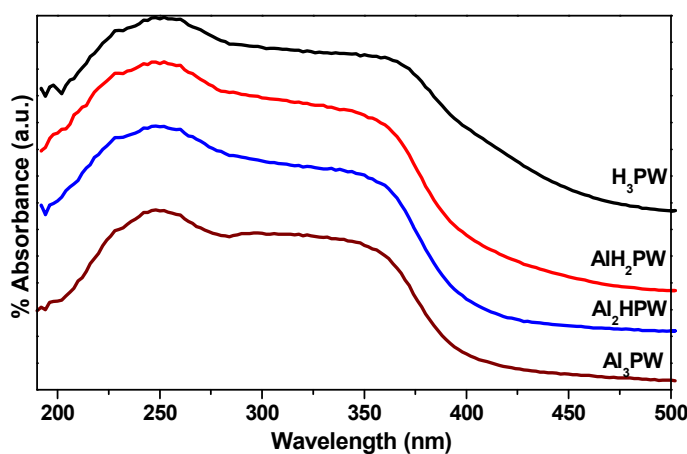

Fig. 4: DR UV-*vis* spectra of all the samples

Fournier et al. [32] reported that the LMCT band shifts towards higher wavelength and it broadens when the size of the counter-ion decreases (H^+), i.e. when their polarization power increases and the relative distance between heteropolyanions decreases (this is the case for parent H_3PW. The AlPW salts containing counter-ion (Al^{3+}), the polarization action is lower and as a consequence, the heteropoly anions are isolated one from another.

3.5 N_2-physisorption

The textural properties of the samples were measured by N_2-physisorption studies. The surface area of AlPW samples increased with Al^{3+} content; rising from 7 m^2 g^{-1} for Al_1PW to 27 m^2 g^{-1} for Al_3PW sample was observed (Table 2). This is consistent with the results observed by Moffat et al. [33], they reported that metal salts of H_3PW have dense porous networks and corresponding higher surface areas than the parent

H$_3$PW. Our results are in accordance with those findings, revealing a significant increase

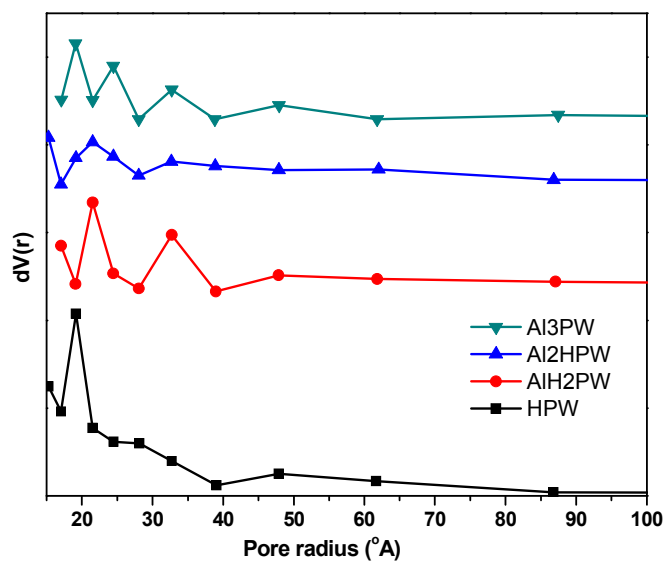in the average pore radius from 20 to 40 Å for AlPW samples (Fig.5).

Fig. 5: Pore size distribution of all the samples

Okuhara et al. [34] showed that large voids exist between the primary particles

(micro crystallites) in these materials. If the size of the primary AlPW clusters is about 12

nm, then the most closely packed aggregates could form voids of around 2-3 nm. Inter

particle voids between larger crystallites would increase the overall apparent average

pore diameter, consistent with the present study.

Table 2: Textural and acidity measurements of the catalysts

Catalyst	N$_2$-physisorption			Total acidity NH$_3$-TPD (mmol/g cat)	FTIR pyridine adsorption		
	S$_{BET}$ (m^2/g)	Pore volume (cc/g)	Average pore radius (Å)		Brönsted acid sites (B)	Lewis acid sites (L)	L/B
HPW	3	0.013	20	1.415	17.6	4.4	0.25
AlH$_2$PW	7	0.018	28	1.154	15.8	6.2	0.39
Al$_2$HPW	12	0.031	35	0.902	14.1	8.1	0.57
Al$_3$PW	27	0.058	50	0.736	13.6	9.7	0.71

3.6 NH$_3$-TPD measurements

Ammonia TPD technique usually enables the determination of the amount of acidic sites and the strength of acid sites present on the catalyst surface together with the total acidity. The NH$_3$-TPD patterns in the temperature range of 100-800 ^{o}C were collected for all the samples are shown in Fig. 6.
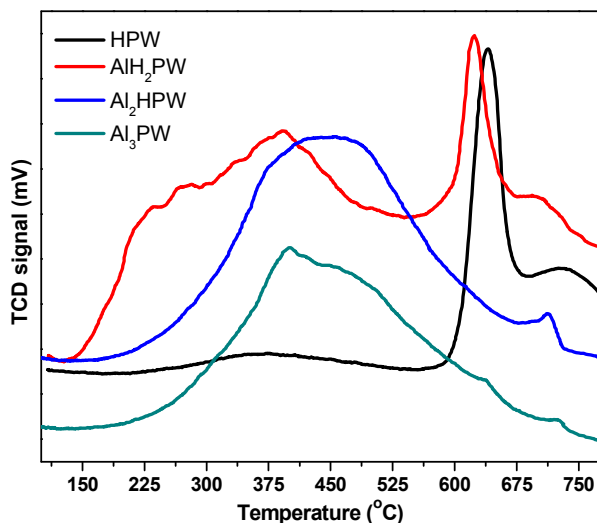

Fig. 6: NH$_3$-TPD patterns of all the samples

The strength of acid sites is related to the corresponding desorption temperature. Generally, the acid sites are classified into the weak (150-300 ^{o}C), medium (300-450 ^{o}C) and strong (450-700 ^{o}C) acid sites [35]. For parent H$_3$PW sample, a small broad hump for medium strength acid sites and two desorption peaks at high temperature (650 ^{o}C and 720 ^{o}C) that were ascribed to strong acidic sites were observed. The NH$_3$ desorption of AlH$_2$PW has the first desorption maximum at 260 ^{o}C (weak acidic sites) and the second peak with the desorption maximum at 385 ^{o}C (strong acidic sites). Ion exchange with one Al atom resulted in shift of the high temperature desorption peaks to lower temperature (620 ^{o}C and 700 ^{o}C). Al$_2$HPW and Al$_3$PW samples showed a major broad peak ranging from 150 to 675 ^{o}C with a small shoulder at 720 ^{o}C.

The TPD profile of dried parent HPW sample was sharp and the desorption takes place in the high temperature region indicating that this sample is energetically homogeneous. Complex desorption profiles were observed for AlPW samples in a broad temperature region (150-750 ^{o}C), composed of at least three overlapped peaks indicate energetic heterogeneity of AlPW salts. This observation is in accordance with the reported results for alkaline metal salts of H_3PW [36].

The total acidity of calculated from TPD analysis was presented in Table 2. The acidity of pure H_3PW is 1.415 mmol per gram of catalyst. Also the total acidity of the strong acidic sites was decreased with increase of Al content. The density of acidic sites on the surface, the highest value, 0.471 mmol/m^2 g cat, was obtained for H_3PW, which was related to its low specific surface area (3.0 m^2/g). Therefore, as expected, the amount and the distribution of the acid strengths on the active phase were significantly influenced by the proton exchange with Al.

3.7 FTIR analysis for pyridine adsorbed samples

The nature of acidic sites such as Brönsted and Lewis acid sites can be distinguished by using pyridine as probe molecule by FTIR studies. It is known that pyridine adsorbed samples exhibit peaks at 1446, 1486 and 1536 cm^{-1}. The peak 1446 cm^{-1} is characteristic of Lewis-coordinated pyridine (L), whereas the band at 1536 cm^{-1} was due to Brönsted -coordinated pyridine (B), and the band at 1486 cm^{-1} is due to Lewis- and Brönsted -coordinated pyridine (L + B) [37].

The FTIR spectra of adsorbed pyridine on parent H_3PW showed typically intense bands at 1485, 1530 and 1541 cm^{-1} that are mainly characteristic of Brönsted type acidity (Fig. 7). In the FTIR spectra of adsorbed pyridine on AlPW samples, new band at 1448

18

cm^{-1} which is attributed to Lewis acid sites was appeared. The intensity of this peak is higher for the Al$_3$PW sample. It can be concluded that compared with parent H$_3$PW sample the Lewis acid sites were introduced by partial exchanging of H with Al ions.
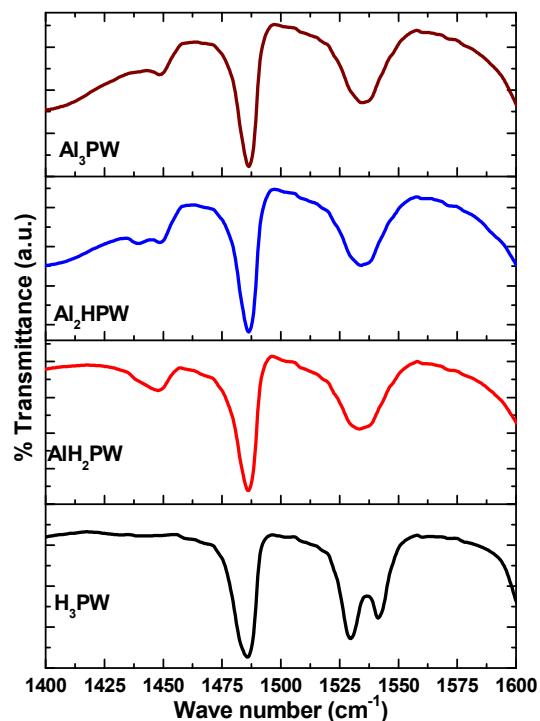

Fig. 7: FTIR analysis for pyridine adsorbed samples

Thus AlPW samples maintained its Brönsted acidity and increased in Lewis acidity, which might be considered as being advantageous for catalyzing the reaction involved in synthesis of pyrido[1,2-*a*]pyrimidine-4-one derivatives. From the above results it can be concluded that partial exchanging of protons with Al ions can introduce Lewis acid sites into pure H$_3$PW molecules and thereby modify the acid strength of parent H$_3$PW *via* Lewis acid sites assisting Brönsted acid sites.

The intensity ratio of B and L acidic sites were calculated from the transmittance intensities at 1536 and 1446 cm^{-1}. With increase in Al^{3+} content, the increase in the Lewis

acidity is much more than the Brönsted acidity and it was observed that Lewis acidity

(L/B = 0.71) maximum for Al_3PW sample.

3.8 Synthesis of pyrido[1,2-*a*]pyrimidin-4-one derivatives

The title compounds were synthesized by a simple and convenient route as
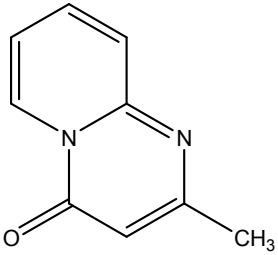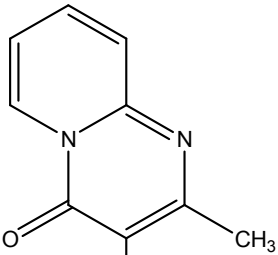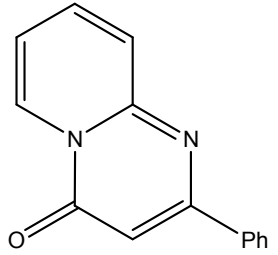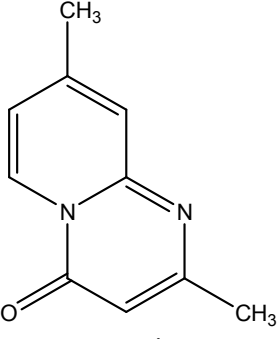
outlined in the Scheme 1.

Table 3: Reaction of $\mathbf{I_a}$ with $\mathbf{II_a}$ in presence of different catalysts under reflux conditions
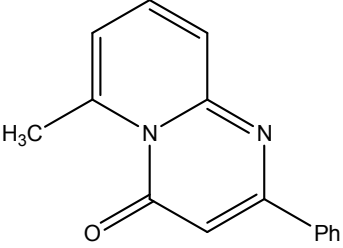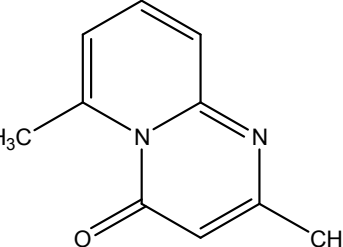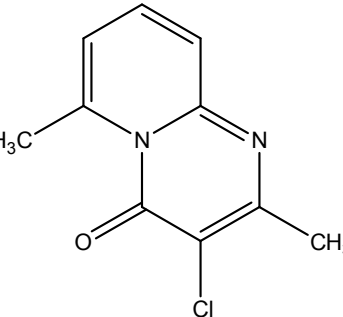
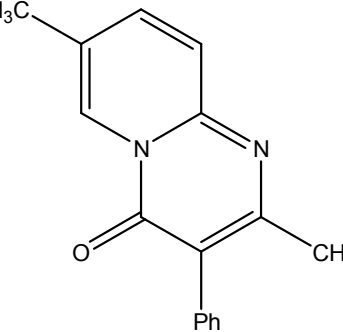| Catalyst	Reaction time* (min.)	Yield (%)
H_3PW	30	40
AlH_2PW	30	67
Al_2HPW	30	81
Al_3PW	18	93

*Reaction conditions: Ethanol solvent (10 ml), 10 mmol of 6-methyl-2-aminopyridine and 10 mmol of 1, 3-dicarbonyl derivatives, 0.1 g ($3.35X10^{-5}$ moles) of catalyst under reflux

The calculated amounts of substituted 2-aminopyridine and 1, 3-di-ketone

derivative were stirred in ethyl alcohol and then the reaction mixture was heated to 80 ^{o}C

to begin the reflux of ethyl alcohol and finally calculated amount of solid heteropolyacid

catalyst was added to the reaction mixture to initiate the reaction. The mixture was kept at

ethanol reflux temperature (80 ^{o}C) until TLC showed no more starting material. The

catalyst was filtered, washed with ethyl alcohol and then the filtrate was taken in a round

bottom flask to remove the alcohol under reduced pressure and the product was

recrystallized to afford the pyrido [1,2-*a*] pyrimidin-4-one derivative.

Table 4: The efficiency of Al₃PW catalyst towards the synthesis of different pyrido [1, 2-*a*] pyrimidin-4-one derivatives.

Compound number	Reaction time* (min)	Yield (%)	Literature yield (%)
III-a	12	96	66 [21]
III-b	20	91	51 [22]
III-c	16	98	81 [21]
III-d	20	93	65 [23]

 III-e	20	96	69 [23]
 III-f	18	93	60 [24]
 III-g	18	91	66 [25]
 III-h	15	96	22 [26]

*Reaction conditions: Ethanol solvent (10 ml), 10 mmol of 6-methyl-2-aminopyridine and 10 mmol of 1,3 dicarbonyl derivatives, 0.1 g (3.35×10^{-5} moles) of Al_3PW catalyst under reflux

In the formation of the pyrido[1,2-*a*]pyrimidine-4-one derivative, the reaction was completed in 30 minutes when H_3PW, AlH_2PW, Al_2HPW were used as catalysts and the reaction time was drastically reduced to 18 minutes in case of Al_3PW catalyst (Table 3).

22

The yield of the product was also depended on the type of the catalyst used. It was found that higher yields were observed in case of Al_3PW catalyst compared to parent H_3PW and other AlPW salts. Recrystallization of the 2, 6-dimethyl-4H-pyrido [1,2-a]pyrimidin-4-one yielded yellow crystals with 93% yield. The products with greater purity were obtained in case of all the catalysts.

The scope and generality of the methodology is illustrated with respect to eight different substituted 1,3-diketone derivatives and the results are presented in Table 2. Interestingly, substituted 1,3-diketone derivatives participated well in the reaction system. The reaction underwent smoothly with different 1,3-diketone derivatives to afford the corresponding substituted-4H-pyrido [1,2-*a*] pyrimidin-4-one derivatives in good yields (entries IIIa-h, Table 4). The yields of 4H-pyrido [1,2-*a*] pyrimidin-4-one derivatives reported in the literature reports are poor (maximum 69%), in comparison the present protocol involved solid Al_3PW catalyst offered very high yields (91 to 98%). The yield of 4H-pyrido [1,2-*a*] pyrimidin-4-one derivative with chlorine moiety is relatively lower than the other derivatives without chlorine group. This could be explained the effect of electron withdrawing ability of chlorine atom.

The synthesized compounds were characterized by IR, ^{1}H and ^{13}C NMR spectral methods. The ^{1}H-NMR spectral data of synthesized compounds displayed characteristic protons of the pyridine nucleus of pyridopyrimidine (C_6-C_9) and the protons of the two methylene groups at 6.71 (supporting information). All the derivatives displayed the characteristic peaks at C_6 -C_9 of the pyridine ring appeared at 7.8, 7.1 and 6.85 respectively. The imine protons present in the derivatives were appeared as singlet at δ 8.4-8.7. The ^{1}H NMR also showed the peaks at δ 3.01 and 3.92 with J = 7Hz for -CH_2

and -OCH$_2$ protons. The data from mass analysis and melting points determined for the synthesized derivatives are in accordance with the values reported in the literature. The elemental microanalyses of the starting materials compounds the derivatives confirmed their chemical structures and were within the acceptable range.
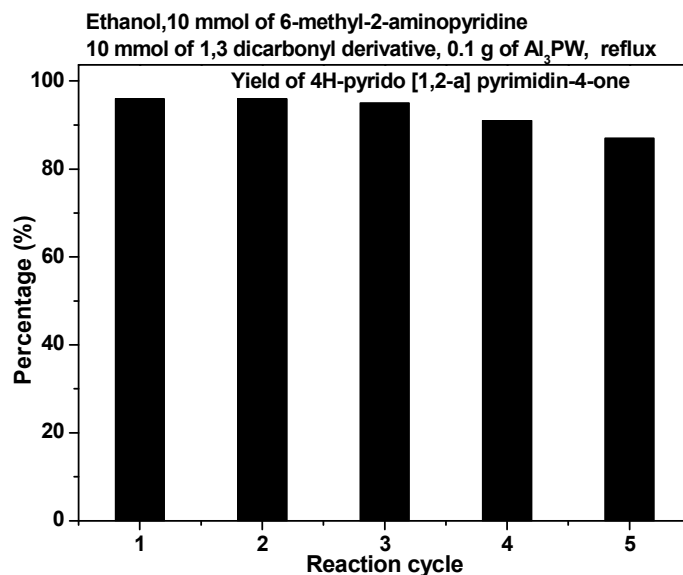

Fig.8: Reusability of Al$_3$PW catalyst for synthesis of 4H-pyrido [1,2-*a*] pyrimidin-4-one

The reusability of the highly active Al$_3$PW catalyst was checked for several reaction cycles (Fig.8), the catalyst removed after the completion of the reaction by filtration, washed with hot ethanol and dried under vacuum. The recovered catalyst was reused for five times using the same reaction conditions. The results showed that the regenerated catalyst performs the reactions efficiently under the same reaction conditions even after being used for five times. The slight decrease in yield observed in the catalytic activity of the Al$_3$PW catalyst on the fourth and fifth time and the decrease of activity could be attributed to the weight loss of the catalyst during the working up in each time. These results are indicating the robust nature of the Al$_3$PW catalyst to synthesize 4H-pyrido [1,2-*a*] pyrimidin-4-one derivatives.

24
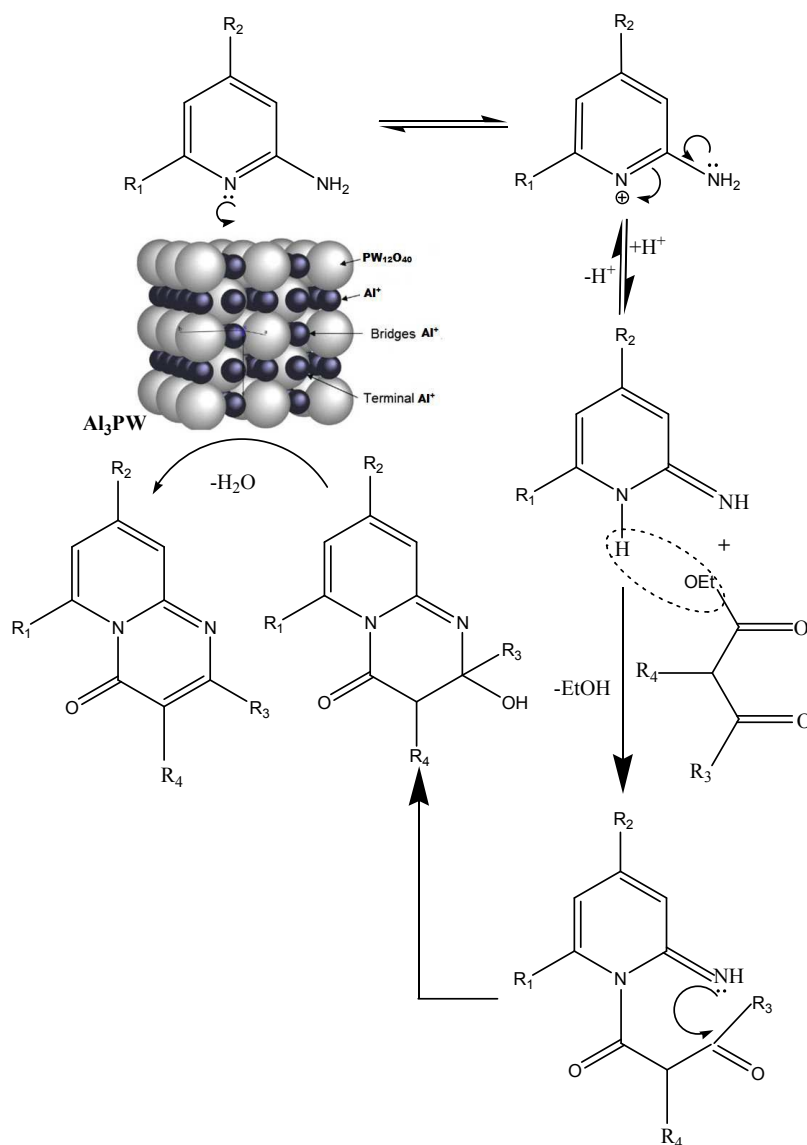
Scheme 2: Plausible mechanism of the reaction between 2-aminopyridine and 1,3-diketone derivative

The plausible mechanism of the reaction between 2-aminopyridine and 1, 3-dicarbonyl derivative is presented in Scheme 2. The interaction between these two molecules is known to proceed through the intermediacy of enamines, which are cyclized to the desired pyridopyrimidines. The nitrogen ring of 2-aminopyridine combined to the double bond of the 1,3-dicarbonyl to give a carbanion intermediate. This carbonion

abstracts a proton from the amino group to give the intermediate enamine product. The intermediate product gives the final product after the catalytic dehydration.

To study the stability of the Keggin structure of the catalysts after the regeneration in each cycle, FTIR spectra of fresh and used Al$_3$PW catalyst were compared (supporting information, Fig. S1). The FTIR spectra of the samples have not showed any major differences in bands at 1080, 981, 886, 791, 593, and 525 cm^{-1}, which corresponds to the characteristic P-O$_a$, W-O$_d$, W-O$_b$-W, W-O$_c$-W stretching vibrations. The results are indicating that Keggin ion was intact in Al$_3$PW catalyst after use of several reaction cycles.

Authors also tested homogeneous acid catalysts such as conc. HCl and conc. H$_2$SO$_4$, which offered mixture of products as these acids known to protonate the multiple carbonyl groups. However, the Al$_3$PW catalyst is selective for protonate single carbonyl carbon to make NH$_2$ attack more favorable. The observed catalytic performance of the catalysts indicates the acidity of the catalyst play a key role in obtaining the highest 4H-pyrido [1,2-*a*] pyrimidin-4-one derivative yield. A through characterization of the catalysts was performed to understand the role of physic-chemical properties of heteropoly acid salts in the catalytic activity.

Conclusions

A simple and efficient synthesis of some substituted pyrido[1,2-*a*] pyrimidin-4-ones derivatives was carried out using Keggin structured AlPW salts as heterogeneous catalysts. The synthesis of pyrido[1,2-*a*] pyrimidin-4-ones derivatives by one-pot two component cyclization of 2-aminopyridine and 1,3-dicarbonyl derivatives using a

catalytic amount of AlPW catalyst at low reaction temperature. This method not only preserves the simplicity, low temperature need, short time, but also consistently gives the corresponding products in excellent yields (90-93%). Among the prepared catalysts, Al_3PW offered high yields of pyrido[1,2-*a*] pyrimidin-4-ones derivatives due to its high surface area and more number of Lewis acid sites.

Acknowledgements

References

[1] R. N. Castle and S. D. Phillips, In Comprehensive Heterocyclic Chemistry; A. R. Katritzky, C. W. Rees, Eds.; Pergamon press: Oxford, 1984; vol. 3, pp 329-368; J. M. Blaney, C. Hansch, C. Silipo and A. Vittoria, *Chem. Rev.* 1984, **84**, 333-407.

[2] J.E. Leysen, P.M. Janssen, A.A. Megens and A. Schotte, *J. Clin. Psychiatry* 1994, **55**, 5-12.

[3] Y. Yanagihara, H. Kasai, T. Kawashima and T. Shida, *Jpn. J. Pharmacol.* 1988, **48**, 91-101.

[4] F. Awouters, J. Vermeire, F. Smeyers, P. Vermote, R. Van Beek and C. J. E. Niemegeers, *Drug Dev. Res.* 1986, **8**, 95-102.

[5] R.L. Smith, R.J. Barrett and E. Sanders-Bush *J. Pharmacol. Exp. Ther.* 1995, **275**, 1050-1057.

[6] I. Devi, J. L. Borah and P. L. Bhuyan, *Tetrahedron Lett.*, 2003, **44**, 8307-8310; Y. Gao, S. J. Tu, T. J. Li, X. J. Zhang, S. L. Zhu, F. Fang and D. Q. Shi, *Synth Commun.*, 2004**, 34**, 1295-1299; Y. L. Li, B. X. Du, X. S. Wang, D. Q. Shi and S. J. Tu, *J. Chem. Res.*, 2006, **2006**, 157-159.

[7] I. Hermecz, J. Kokosi, B. Podanyi and Z. Liko, *Tetrahedron* 1996, **52**, 7789-7796; P.L. Ferrarini, C. Mori, F. Mori, G. Saccomanni, S. Barontini, M. Macchia, P. Barili and M. Hamdan, *J. Heterocycl. Chem.* 1999, **36**, 1065-1072; L. Selic, S. Strah, R. Toplak and B. Stanovnik, *Heterocycles* 1998, **47**, 1017-1022; L. Selic and B. Stanovnik, *J. Heterocycl. Chem.* 1997, **34**, 813-816; A. Bowler, A. Dinsmore, P. Doyle and D. Young, *J. Chem. Soc., Perkin Trans. 1,* 1997, 1297-1306.

[8] G. Roma, M. B. DiBraccio, A. Albi, M. Mazzei and A. Ermili, *J. Heterocyclic Chem.* 1987, **24**, 329-335.

[9] G. J. S. Doad, D. I. Okor, F. Scheinmann, P. A. Bates and M. B. Hursthouse, *J. Chem. Soc.,Perkin Trans 1,* 1988, 2993-3003.

[10] V. A. Dorokhov, S. V. Baranin, A. Dib, V. S. Bogdanov, I. P. Yakovlev, G. A. Stashina and V. M. Zhulin, *Chem. Abstr.* 1991, **114**, 101911.

[11] O. P. Suri, K. A. Suri, B. D. Gupta and N. K. Satti, *Synth. Commun.* 2002, **32**, 741-746.

[12] G. C. B. Harriman, S. Chi, M. Zhang, A. Crowe, R. A. Bennett and I. Parsons, *Tetrahedron Lett.* 2003**, 44**, 3659-3661.

[13] J. H. Clark, *Acc. Chem. Res.* 2002, **35**, 791-797.

[14] I. V. Kozhevnikov, *Catal. Rev. Sci. Eng.* 1995, **37**, 311-352.

[15] M. Misono, *Catal. Rev. Sci. Eng.* 1988, **30**, 339-392.

[16] T. Okuhara, N. Mizuno and M. Misono, *Adv. Catal.* 1996, **41**, 113-252.

[17] M. Misono, *J. Chem. Soc., Chem. Commun.,* 2001, 1141-1152.

[18] T. Baba, H. Watanabe and Y. Ono, *J. Phys. Chem.* 1983, **87**, 2406-2411.

[19] H. Firouzabadi, N. Iranpoor, F. Nowrouzi, and K. Amani, *Chem. Commun.* 2003, 764-765.

[20] K. Narasimharao, E. Al-Sabban, T. S. Saleh, A. G. Gallastegui, A. C. Sanfiz, S. Basahel, S. Al-Thabaiti, A. Alyoubi, A. Obaid and M. Mokhtar, *J. Mol. Catal. A: Chem.* 2013, **379**, 152-162; T. S. Saleh, K. Narasimharao, N. S. Ahmed, S. N. Basahel, S. A. Al-Thabaiti and M. Mokhtar, *J. Mol. Catal. A: Chem.* 2013, **367**, 12-22; M. Mokhtar, T.S. Saleh and S.N. Basahel, *J. Mol. Catal. A: Chem.* 2012, **353-354**, 122-131.

[21] H.G. Bonacorso, F. J. Righi, I. R. Rodrigues, C. A. Cechinel, M. B. Costa, A. D. Watsowski, M. P. Martins and N. Zanatta, *J. Heterocyclic Chem.*, 2006, **43**, 229-233.

[22] M. Shur and S. S. Israelstem, *J. Org. Chem.*, 1968, **33**, 3015-3020.

[23] P. L. Ferrarini, C. Mori, O. Livi, G. Biagi and A. M. Marini, *J. Heterocyclic Chem.*, 1983, **20**, 1053-1057.

[24] J.C. Christopher, W. D. Leslie and A. R. James and T. Vasilios, *J. Heterocyclic Chem.* 1982, **19**, 1017-1019.

[25] L. F. Pier, C. Mori, O. Livi, G. Biagi and A. M. Marini, *J. Heterocyclic Chem.* 1983, **20**, 1053-1057

[26] N. Sin, A. C. Good, B. L. Venables, P. M. Scola, N. A. Meanwell, *US patent* 2006, 183694

[27] K. Narasimharao, D.R. Brown, A.F. Lee, A.D. Newman, P.F. Siril, S.J. Tavener and K. Wilson, *J. Catal.* 2007, **248**, 226-234.

[28] J.A. Dias, E. Caliman and S. C.L. Dias, *Micro. Meso. Mater.* 2004, **76**, 221-232.

[29] P. M. Rao, P. Goldberg-Oppenheimer, S. Kababya, S. Vega and M. V. Landau, *J. Mol. Catal. A: Chem.* 2007, **275**, 214-227.

[30] M.T. Pope, Heteropoly and Isopoly Oxometalates, Springer-Verlag, Berlin, 1983.

[31] Y. Miao, G. Lu, X. Liu, Y. Guo, Y. Wang and Y. Guo, *Micro. Meso. Mater.* 2009, **122**, 55-60.

[32] M. Fournier, C. Louis, M. Che, P. Chaquin and D. Masure, *J. Catal.* 1989, **119**, 400-414.

[33] J.B. Highfield, B.K. Hodnett, J.B. McMonagle and J.B. Moffat, Proc. 8th Int. Congr. Catalysis, vol. 5, ed. IUPAC, Verlag Chemie, Frankfurt AM Main, 1984, p. 611.

[34] T. Okuhara, T. Nishimura, H. Watanabe and M. Misono, *J. Mol. Catal.* 1992, **74**, 247-256.

[35] F. Jing, B. Katryniok, E. Bordes-Richard and S. Paul, *Catal. Today* 2013, **203**, 32-39.

[36] L. Damjanovica, V. Rakic, U.B. Mioc and A. Auroux, *Thermochimica Acta* 2005, **434**, 81-87.

[37] T. T. Ali, K. Narasimharao, N. S. Ahmed, S. Basahel, S. Al-Thabaiti and M. Mokhtar, *Appl. Catal. A: Gen.* 2014, **486**, 19-31.

Graphical Abstract

a, $R_1=CH_3$ $R_2=H$
b, $R_1=CH_3$ $R_2=Cl$
c, $R_1=Ph$ $R_2=H$